Nonlinear Absorption Properties and Excited State Dynamics of Ferrocene

Stefano Scuppa, Laura Orian, Danilo Dini, Saverio Santi, and Moreno Meneghetti*

Department of Chemical Sciences, University of Padova, Via Marzolo 1, I-35131 Padova, Italy

Received: May 20, 2009; Revised Manuscript Received: July 3, 2009

We report on the first observation of reverse saturable absorption by ferrocene (Fc) in toluene using nanosecond pulses at 532 nm. Pump and probe experiments in the visible spectral region show the existence of an excited triplet state with an intersystem crossing quantum yield $S_1 \rightarrow T_1$ of 0.085 and a molar extinction coefficient ε_{Fc}^{T} of 5650 L mol^{-1} cm^{-1} at 700 nm. The full understanding of the nonlinear optical behavior of Fc cannot be obtained, however, with a model that includes only the one-photon absorption from T_1, but it is mandatory to consider also a simultaneous two-photon absorption from an excited singlet state of Fc (two-photon absorption cross section: 2.4×10^{-41} cm^4 s ph^{-1} mol^{-1}). The optical spectrum of the ground and triplet state of Fc are calculated within a TD-DFT approach considering several functionals (PBE, BLYP, LDA, OPBE) for the optimization of molecular geometry.

Introduction

Ferrocene (Fc) [iron *bis*-cyclopentadienyl (Cp)] with its unintentional synthesis in the early fifties[1] constitutes one of the first examples of organometallic compounds for the presence of direct bonds between carbon atoms and iron.[2] The combination of high chemical and photochemical stability,[3] which are typical of aromatic compounds, with the richness of the redox chemistry for the presence of a metallic atom, has made Fc and its derivatives a particularly popular class of materials in electrochemistry,[4] photochemistry[5] and photophysics.[6] The frontier π-orbitals of the cyclopentadienyl rings and the metal d orbitals are responsible for the sandwich-shaped geometry of iron coordination. Such a structure strongly influences the chemical reactivity of Fc[7] and determines its photochemical and photophysical properties.[8]

Excited Fc showed to relax into a triplet state and the value of the intersystem crossing $S_1 \rightarrow T_1$ quantum yield (ϕ_{ISC}) was found to be 0.66 in DMSO by the indirect method of Fc-sensitized photoisomerization of phenylosazone-D-glucose.[9] By using Fc as triplet quencher, the energy value of its first excited triplet state T_1 was estimated 39−41 kcal mol^{-1} (1.7−1.8 eV) above the ground state.[6b−e] The direct measurement of the lifetime of Fc in the first excited singlet state S_1 and triplet state T_1 by flash photolysis[6c,e] and laser flash photolysis[6d,10] was not possible as well as the direct determination of $T_1 \rightarrow T_2$ transient absorption.[6d,e,10] The lifetime of T_1 in DMSO was obtained only through the same indirect method used for the evaluation of ϕ_{ISC} and was found to be 0.6 ns.[11] The possible existence of a phosphorescence spectrum of Fc has been the object of several studies, but the presumed phosphorescent nature of the first observation of emission[12,13] was successively corrected.[14] It is now generally accepted that Fc is not phosphorescent. Fluorescent emission of Fc between 402 and 574 nm[15] has been reported in one case and was not further confirmed.

In the field of nonlinear optics, Fc has mainly played the role of electron donor in charge transfer processes within dyads where Fc was covalently linked to an acceptor like fullerene, porphyrins, and linear π-conjugated systems.[7,16] In these compounds the observation of nonlinear optical (NLO) effects has been related to the electron acceptor moiety of the dyad because of its overwhelming polarizability.[7,16] In other situations the Fc triplet was considered important for the excited state dynamics in particular for the competition between energy and charge transfer processes.[17] However, the evaluation of the triplet state and of the NLO properties of sole Fc could not be obtained.

In the present contribution, we report on the NLO absorption properties of neutral Fc in toluene excited at 532 nm with nanosecond laser pulses. Pump and probe measurements show that Fc excited states, with lifetime of the order of some tenth of nanoseconds, are present in the nonlinear process. The fact that Jaworska-Augustyniak et al., who measured the intersystem crossing quantum yield,[9] were not able to see a transient spectrum in the nanosecond time regime measurements can be understood considering both the lower energetic pulses of their experiments and the different solvent (DMSO) they used. In fact DMSO, probably due to the presence of an S atom, has a stronger interaction with Fc, as one can also see in the variation of its linear spectrum with respect to that of the toluene solution, and determines faster excited state decay rates, which do not allow to see transient absorptions in the nanosecond regime, as we also verified.

The transient excited state reported in the present paper is determined to be a triplet since we observe the same transient absorption by exciting a solution (toluene and 10% ethanol) of eosin-Y and Fc, for which it is known that a triplet−triplet energy transfer from eosin to Fc occurs.[6c] A value of the molar extinction coefficient $\varepsilon_{Fc}^{T} = 5650$ L mol^{-1} cm^{-1} at 700 nm and an intersystem crossing quantum yield $\phi_{ISC} = 0.085$ are obtained for the triplet using a pump and probe comparative method, as described in the experimental section.[18] The different ϕ_{ISC} value we find with respect to the previous determination (0.66)[9] can be again attributed to the different excited state dynamic induced by the Fc-DMSO interaction.

TD-DFT[19] calculations allowed us to account for both the linear ground state optical spectrum and the linear triplet transient spectrum. Modeling of the nonlinear absorption properties is obtained solving[20] kinetic equations for the excited states population dynamic, namely, for the time dependent diagonal part of the density matrix.

* Corresponding author. E-mail: moreno.meneghetti@unipd.it.

10.1021/jp9047192 CCC: $40.75
Published on Web 07/24/2009

We found that the nonlinear transmission variations we measured cannot be simply explained considering the triplet excited state of Fc because of the low ϕ_{ISC} and the small ε^{T}_{Fc}. Similar to the cases of hemiporphyrazines[21] and $(TMTTF^{+})_2$[22], it is found that nonlinear transmission curves are best fitted when a two-photon-absorption process from the excited singlet state is also considered.

Experimental Section

Ferrocene was purchased by Fluka (≥98%) and sublimed two times under vacuum.

Absorption spectra of Fc have been recorded with a Varian Cary 5 UV−visible spectrophotometer using 10 mm quartz cells. Fluorescence spectra have been recorded with a FluoroLog-3 spectrometer (Horiba Jobin Yvon), and fluorescence lifetimes were obtained using a time correlated single photon counting (TCSPC) technique with the same instrument. For the TCSPC measurement, samples were excited at 375 nm with pulses of 1.3 ns obtained by a diode led (nanoled Horiba Jobin Yvon).

All calculations were performed with the Amsterdam Density Functional (ADF) program.[23] The large uncontracted set of Slater-type orbitals (STOs) TZ2P[24] was used. The TZ2P basis is of triple-ζ quality, augmented by two sets of polarization functions. The frozen core approximation was used for the core electrons: up to 1s for C and up to 2p for Fe.[25] An auxiliary set of STOs was used to fit the molecular density and to represent the Coulomb and exchange potentials accurately in each SCF cycle. Scalar relativistic corrections were included using the zero order regular approximation (ZORA).[26] Energies and gradients were calculated using (i) local density approximation (LDA) and Slater exchange and VWN correlation,[27] (ii) BLYP Becke exchange[28] and LYP correlation,[29] (iii) PBE, exchange, and correlation terms proposed by Perdew-Burke-Ernzerhof,[30] and (iv) OPBE[31] and LDA approximation with nonlocal corrections due to Handy-Cohen[32] and Perdew−Burke−Ernzerhof correlation.[30] TD-DFT calculations were carried out on the PBE optimized geometry using all electron TZ2P basis sets for all of the atoms and including both scalar relativistic[25] and spin orbit relativistic effects.[33] The exchange correlation (XC) functional of Van Leeuwen and Baerends (LB94)[34] was employed.

Nonlinear transmission curves of Fc were recorded at 532 nm in an open-aperture configuration as a function of the incident energy of 9 ns laser pulses of a doubled Nd:YAG laser (Quantel YG980E) at the repetition rate of 1 Hz. Intensity of the incident pulses was controlled with a $\lambda/2$ wave plate and a polarizing cube beam splitter. The laser pulse area on the sample was 0.030 cm^2, and the solvents were fluxed with nitrogen for 5 h prior any measurement. Glass cells with 2 mm optical path were used for the measurements. The intensity transmitted by the sample was recorded by a pyroelectric detector (Scientech Mod. SPHD25) and normalized, pulse by pulse, with a calibrated photodiode.

Lifetime and absorbance of Fc excited states were determined with pump and probe experiments. Comparison of the linear optical spectra of the solutions before and after the pump and probe measurements did not reveal photodegradation of Fc showing the very high stability of this molecule. The same pulses used for the NLO transmission measurements were used for the pump and probe experiments but with a pulse area on the sample of 0.12 cm^2 so that the probe spot was well inside the pump area. A continuous Xe lamp from Spectra-Physics (Oriel Instruments, Mod. 66902, 150 W) was used as a probe. The variation of sample transient transmission was detected by a Horiba Jobin-Yvon TRIAX 320 spectrometer equipped with a Hamamatsu phototube (R2257). The temporal variation of the phototube signal was averaged by a 1-GHz digital oscilloscope (LeCroy LC564A) on a microsecond time scale with nanosecond resolution. Solvents were fluxed with nitrogen 5 h prior any measurement.

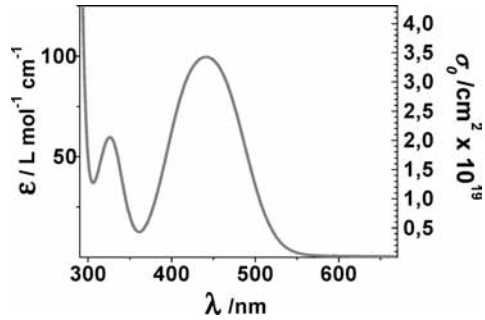

Figure 1. Molar extinction coefficient, ϵ, and ground state absorption cross-section, σ_0, for Fc in toluene in the UV−visible range.

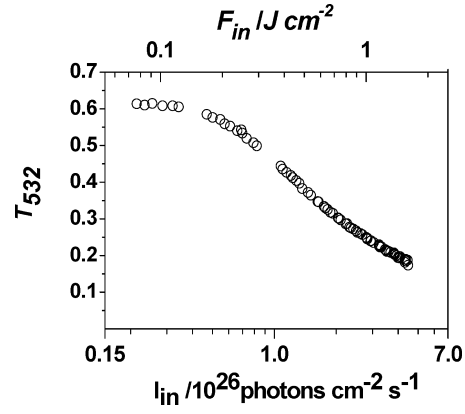

Figure 2. Nonlinear transmission of Fc in toluene at 532 nm. Linear transmittance at 532 nm was 0.61.

Results and Discussion

The linear absorption spectrum of Fc in toluene is reported in Figure 1 and it does not show signs of aggregation of the molecules.

In the near UV−visible range, Fc presents two main absorption peaks at 330 and 441 nm. The peak at lower energies includes a tail of absorption that extends to 600 nm. This allows an efficient pumping of the system at 532 nm, that is, the wavelength of the duplicated Nd:YAG laser.

Fc ($C = 0.16$ M in toluene) behaves as a reverse saturable absorber[35] when irradiated with nanosecond pulses at 532 nm (Figure 2). In fact, the nonlinear transmission decreases for incident fluences (F_{in}) increasing up to 2.0 J cm^{-2}. We found a complete recover of the initial transmittance value (T_0) for decreasing fluences. This shows that, in comparison to other classes of reverse saturable absorbers,[36] Fc has a high photostability.

The stability is also proved by the absence of spectral variation of the UV−visible spectrum taken before and after the nonlinear transmission measurements.

The limiting threshold fluence F_{lim}, defined as the fluence at which the transmittance is half the linear one,[38] is found to be 0.7 J cm^{-2}. This value is higher than that of fullerene ($F_{lim} =$ 0.1 J cm^{-2})[39] and other molecular systems[35−38] when linear transmittance is the same.

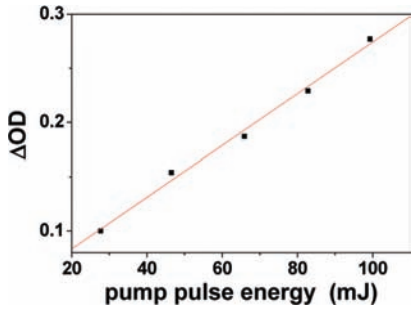

Figure 3. Differential optical densities recorded at 700 nm as a function of the energy of the pump pulses.

Occurrence of reverse saturable absorption (RSA) of nanosecond pulses shows that the excited electronic states of Fc involved in the NLO effect possess larger absorption cross sections, σ_{exc}, with respect to the ground state [σ_0 (532 nm) = 2.2×10^{-20}cm^2]. We used pump and probe experiments, in the nanosecond time regime, to determine the lifetimes and dynamics of excited states.

By using the same laser pulses of the nonlinear transmittance measurements, but with a larger pump area on the sample (see experimental section), we recorded, for Fc in toluene [$C = 0.16$ M; T_0 (532 nm) = 0.61], low intensity transient differential optical density signals in the visible and near-infrared spectral region. Since Fc is very stable under laser irradiation, we were able to record signals with high differential optical densities but always in a linear regime as shown in Figure 3.

Figure 4 shows some of the recorded transient signals using $F_{in} = 1.1$ J cm^{-2} in a temporal range of 1 μs. Fitting of the data can be obtained with a biexponential decay with time constants of 26 ± 10 and 164 ± 10 ns. This indicates that more than one excited state is involved in the decay process.

Transient spectra are obtained at different time intervals with respect to the laser pulse (Figure 5). The spectra show an increasing intensity in the short wavelength region without any band in the visible and near-infrared. Moreover, they do not show any evolution with time, indicating that other transient species are not formed during the RSA process.

Both spectra, obtained from the fast and slow component of each transient signal (not shown here), present the same unstructured profile that is characterized by the lack of any absorption band in the analyzed range.

In order to identify the excited state generating the transient spectrum of Figure 5, we used eosin-Y, which is known to populate the triplet state of Fc by a triplet to triplet energy transfer process.[6c] For the characterization of the triplet state of Fc and, in particular, to obtain the intersystem crossing quantum yield, we performed experiments with a variable concentration of Fc with respect to eosin-Y. We used a toluene/ethanol (9/1 v/v) solution of eosin-Y ($1.5\ 10^{-5}$ M) and Fc in large excess. The measured ΔOD at 700 nm, a wavelength at which only the excited states of Fc absorb, can be considered the sum of two contributions: ΔOD_{Eos} which is due to the absorption of the excited state of Fc produced by triplet energy transfer from eosin-Y, and ΔOD_{Fc} which represents the absorption of the transient species generated upon direct excitation of Fc. The possible observation of a transient signal at 700 nm is attributed to Fc triplet because the same concentration of eosin-Y excited in the same conditions does not give any transient absorption signal at this wavelength.

Because of the large concentration of Fc, we consider that eosin-Y generates the Fc triplet with full efficiency. Therefore, we can write:

$$\Delta OD_{Eos-Fc} = \Delta OD_{Eos} + \Delta OD_{Fc} = \phi_{Eos}^{ISC} C_{Eos}^{1} \varepsilon_{Fc}^{T} d + \phi_{Fc}^{ISC} C_{Fc}^{1} \varepsilon_{Fc}^{T} d \quad (1)$$

where ϕ_{Eos}^{ISC} and ϕ_{Fc}^{ISC} are the intersystem crossing quantum yield for eosin-Y and Fc, C_{Eos}^{1} and C_{Fc}^{1} are the first singlet excited state (S_1) molar concentration of eosin-Y and Fc generated by a laser pulse, ε_{Fc}^{T} is the molar extinction coefficient for the Fc triplet, and d is the cell thickness. Since the concentration of eosin-Y is constant and the concentration of the first excited singlet of Fc is proportional to its ground state concentration (C_{Fc}^{0}), one can write:

$$\Delta OD_{Eos-Fc} = aC_{Fc}^{0} + b \quad (2)$$

Considering the excited state concentration dependence on the pulse intensity,[40] one finds:

$$\phi_{Fc}^{ISC} = \phi_{Eos}^{ISC} C_{Eos}^{0} (\varepsilon_{Eos} a / \varepsilon_{Fc} b) \quad (3)$$

where C_{Eos}^{0} is the ground state concentration of eosin-Y, and ε_{Eos} and ε_{Fc} are the ground state extinction coefficients of eosin-Y and Fc. In Figure 6 are reported the intensities of the maximum value of the measured ΔOD at 700 nm as a function of the concentration of Fc. One finds a linear dependence, and the values of $a = 1.05$ L mol^{-1} and $b = 0.28$.

We found that the quantum yield of fluorescence $\phi_{Eos}^{F} = 0.27$ for eosin-Y in a toluene/ethanol (9/1 v/v) solution by the

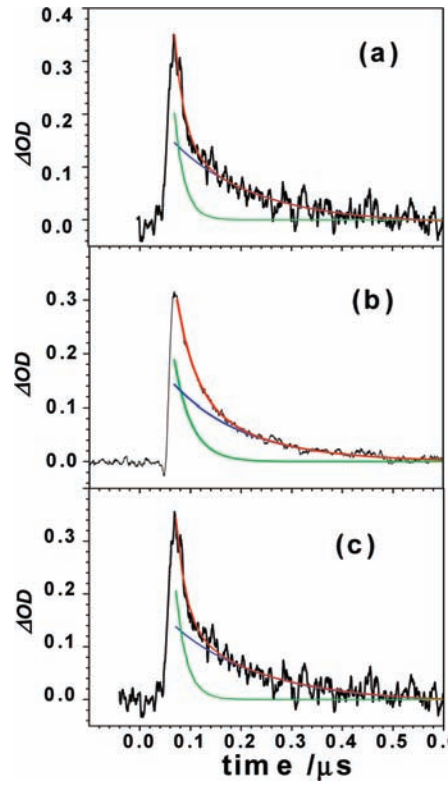

Figure 4. Temporal variations of differential optical densities for Fc in toluene (C, 0.16 M; cuvette thickness, 2 mm) at 505 (a), 580 (b), and 820 (c) nm. Temporal profiles are averages of 200 consecutive traces. Excitation wavelength: 532 nm; $F_{in} = 1.1$ J cm^{-2}. Fittings (red curves) have been obtained with a biexponential decay and time constants of 26 ± 10 ns and 164 ± 10 ns. Blue and green curves refer to the monoexponential components of the resulting fitting.

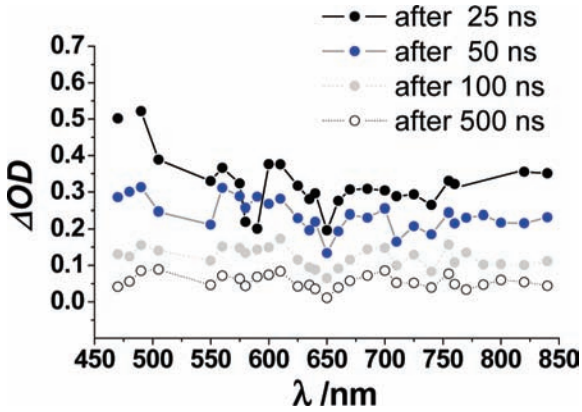

Figure 5. Transient spectra of Fc in toluene ($C = 0.16$ M; cuvette thickness, 2 mm). Excitation wavelength, 532 nm; frequency of irradiation, 1 Hz; $F_{in} = 1.1$ J cm^{-2}.

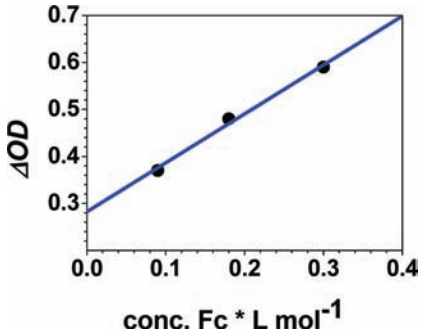

Figure 6. ΔOD and linear fitting of the solutions of 1.5 10^{-5} M eosin-Y and Fc with $C = 0.09$, 0.18, 0.30 M in toluene/ethanol (9/1 v/v) at the maximum peak height (probe $\lambda = 700$ nm). Each point was averaged using 40 pulses.

comparative method,[41] using as a reference the same eosin-Y in 95% ethanol solution of KOH 0.01 M ($\phi^{F}_{Eos} = 0.65$). By assuming that internal conversion is always much slower than ISC for eosin-Y,[42] we find that $\phi^{ISC}_{Eos} = 1 - \phi^{F}_{Eos} = 0.73$. Therefore, from eq 3, we find that $\phi^{ISC}_{Fc} = 0.085$.

For the determination of ε^{T}_{Fc} in toluene, we compared the triplet absorption of fullerene C_{60} in toluene at 745 nm with that of Fc at 700 nm. We recorded the transient triplet−triplet absorption of C_{60} ($\Delta OD_{C60} = 0.64$) exciting the solution ($T_0(532) = 0.80$), with laser pulses of 27.8 mJ, and recorded the transient signal for Fc ($\Delta OD_{Fc} = 0.136$) exciting the solution ($T_0(532) = 0.56$) with laser pulses of 83.7 mJ. It is known that for C_{60} in toluene $\varepsilon_{C60} = 15000$ L mol^{-1} cm^{-1} and ϕ^{ISC}_{C60} is close to 1.[43] With the following expression:

$$\frac{\Delta OD_{C60}}{\Delta OD_{Fc}} = \frac{\phi^{ISC}_{C60}(1 - T)_{C60}E_1\varepsilon_{C60}}{\phi^{ISC}_{Fc}(1 - T)_{Fc}E_2\varepsilon_{Fc}} \quad (4)$$

which also considers that the solutions are absorbing differently and that the exciting pulses have different energies (E_i), we obtained $\varepsilon_{Fc} = 5650$ L mol^{-1} cm^{-1} to which corresponds $\sigma_T = 2.1\ 10^{-17}$ cm^{-2}.

To account for the observed transient spectrum, we performed calculations of the ground and excited state electronic properties. The visible spectrum of Fc in toluene is characterized by the presence of two low intensity absorption bands (molar extinction coefficient $\varepsilon < 10^2$ M^{-1} cm^{-1}) at 325 nm (3.82 eV) and 441 nm (2.81 eV; Figure 1).[44] The origin of the weak absorption bands of Fc in the visible spectrum is associated to spin-allowed transitions between d orbitals of central iron,[8a] the energy of which is perturbed by cyclopentadienyl ligands.[45]

In the following computational analysis, the main features of the electronic spectrum of Fc are revisited through time-dependent density functional theory (TD-DFT) methods[19] with the inclusion of scalar and spin−orbit relativistic effects. Numerous calculations have been performed to describe the geometric and electronic features of this prototypical metallocene compound. The theoretical determination of the equilibrium geometry of Fc is a challenging issue[46] since the calculated metal−ligand distance is often in very poor agreement with the experimental value ($d = 1.65-1.66$ Å).[47] It has been observed that slight geometry modifications greatly affect the subsequent calculation of excitation energies[48] and popular functionals like B3LYP perform poorly in the case of Fc. For this reason, we have tested several functionals, that is, PBE, BLYP, LDA, and OPBE. In particular, PBE has already proved to be efficient in determining the ground state geometric and electronic structure of metallocenes.[30] In all cases, the full geometry optimization converged to an eclipsed Fc with D_{5h} symmetry, which is in agreement with the experiment[34] and with the recent CCSD(T) results by Coriani et al.[49] The metal-ring distance at the different levels of theory is reported in Table 1. The best agreement with the experimental geometry is obtained with PBE functional; thus, the PBE optimized geometry was mainly employed for the subsequent TD-DFT calculations.

The energies of the upper valence Kohn−Sham molecular orbitals of the ground state of Fc, shown in Figure 7, are reported in Table 1.

The order of the highest occupied frontier MOs varies with the functional: while with PBE and BLYP, a_1' (d_{z2}, σ) lies at a lower energy than e_2' (d_{x2-y2},d_{xy}, δ), with OPBE $a_1' \approx e_2'$, and with LDA, e_2' is more stable than a_1', as predicted by crystal field theory.[50] Notably, all of the calculations show that the Fe d orbital percentage of these MOs differ significantly (Table 1). The main contribution to the stability comes from the inner bonding level formed by the $e_1''(\pi)$Cp orbitals with the d_{xz},d_{yz} orbitals of iron. The HOMO−LUMO gap between nonbonding completely occupied orbitals a_1' and e_2' and the empty antibonding e_1'' orbitals is quite large; thus, Fc has a low spin configuration, in agreement with previous results.[51]

The electronic spectrum of Fc, together with the spectra of other metallocenes, was theoretically computed through semiempirical molecular orbital calculations by Armstrong et al.[52] The calculations of the excited states of Fc using the singly excited configuration interaction (CI) and SCF methods have been reported later by Rohmer et al.[53] Boulet[54] employed TD-DFT methods to assign the absorption bands of Fc quite in accord with the experiment and, despite the fact that functionals show some problems in reproducing charge transfer excitations and that novel schemes are an important field of theoretical investigation,[55] he found that LB94 functional performs rather well when a LDA optimized geometry is used; in these calculations, scalar relativistic effects were included within ZORA.[27]

In Table 2 and Figure 8, the visible absorption spectrum of Fc is reported together with the computed excitations and assignments at ZORA LB94 TZ2P all electron level of theory.

As one can observe from Table 2, the best results have been obtained with the PBE optimized geometry, according to previous reports that demonstrate how small changes in the Fe-Cp distance determine large variations in the calculated spec-

TABLE 1: Relevant Structural and Electronic Fc Parameters Optimized with Different Functionals

	ZORA PBE/TZ2P small core			ZORA BLYP/TZ2P small core			ZORA LDA/TZ2P small core			ZORA OPBE/TZ2P small core		
d_{Fe-Q}[a]	1.636			1.687			1.589			1.589		
MO	a_1'	e_2'	e_1''	a_1'	e_2'	e_1''	e_2'	a_1'	e_1''	e_2'	a_1'	e_1''
energy[b]	−4.22	−4.08	−1.13	−4.09	−3.77	−1.15	−4.49	−4.44	−1.25	−4.10	−4.09	−0.83
HOMO−LUMO[b]	2.95			2.62			3.19			3.26		
Fe%[c]	88%	79%	55%	89%	81%	57%	78%	87%	52%	76%	86%	52%
occ	2	4	0	2	4	0	4	2	0	4	2	0

[a] Q denotes the centroid of the Cp ring; values are in Å. [b] Values in eV. [c] Fe d orbital contribution to the MO.

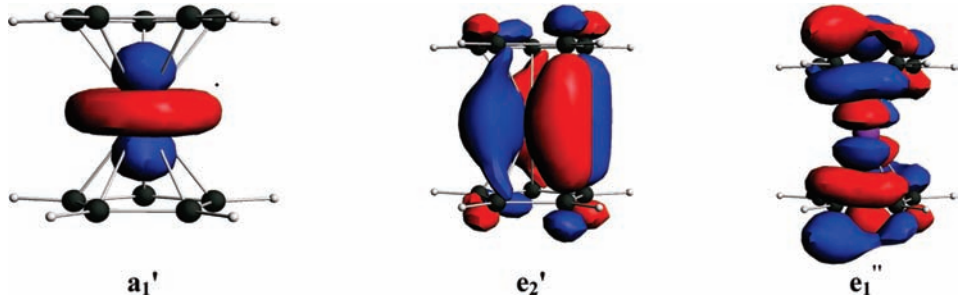

Figure 7. Frontier Kohn−Sham molecular orbitals. Level of theory: ZORA PBE/TZ2P small core. Density: 0.05 (e a_0^{-3})$^{1/2}$.

TABLE 2: Excitation Energies Calculated for Different Optimized Geometries; Level of Theory: ZORA LB94 TZ2P All Electron Basis Set[b]

exc state	ZORA PBE/ LB94	ZORA BLYP/ LB94	ZORA LDA/ LB94	ZORA OPBE/ LB94	exp	assignment
E_2''	2.81 $4e_2' \rightarrow 5e_1''$ (100%)	2.46 $4e_2' \rightarrow 5e_1''$ (100%)	3.18 $4e_2' \rightarrow 5e_1''$ (100%)	3.18 $4e_2' \rightarrow 5e_1''$ (100%)	2.81/2.70[a]	$d_{xy,x2-y2} \rightarrow d_{xz,yz}$
E_1''	2.91 $8a_1' \rightarrow 5e_1''$ (78%) $4e_2' \rightarrow 5e_1''$ (22%)	2.62 $8a_1' \rightarrow 5e_1''$ (72%) $4e_2' \rightarrow 5e_1''$ (28%)	3.21 $8a_1' \rightarrow 5e_1''$ (82%) $4e_2' \rightarrow 5e_1''$ (18%)	3.19 $8a_1' \rightarrow 5e_1''$ (82%) $4e_2' \rightarrow 5e_1''$ (18%)	2.81/2.98[a]	$d_{z2} \rightarrow d_{xz,yz}$, $d_{xy,x2-y2} \rightarrow d_{xz,yz}$
E_1''	3.44 $4e_2' \rightarrow 5e_1''$ (78%) $8a_1' \rightarrow 5e_1''$ (22%)	3.11 $4e_2' \rightarrow 5e_1''$ (71%) $8a_1' \rightarrow 5e_1''$ (28%)	3.77 $4e_2' \rightarrow 5e_1''$ (81%) $8a_1' \rightarrow 5e_1''$ (18%)	3.76 $4e_2' \rightarrow 5e_1''$ (82%) $8a_1' \rightarrow 5e_1''$ (17%)	3.82/ 3.82[a]	$d_{xy,x2-y2} \rightarrow d_{xz,yz}$, $d_{z2} \rightarrow d_{xz,yz}$

[a] From ref 8a. [b] Values are in eV.

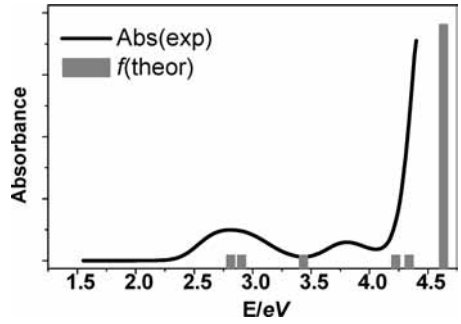

Figure 8. Calculated oscillator strength *f* (gray bars) of the electronic transitions between frontier orbitals of Fc compared with the experimental absorbance (continuous line).

trum.[54] Since spin−orbit coupling is not expected to be relevant in a complex of a metal of the first row, the spin orbit ZORA results (Table 3) are not very different from those reported in Table 2. Nonetheless, they allowed us to identify the spin-forbidden singlet−triplet transition at 2.31 eV reported by Armstrong et al.[44b] The calculation shows that two triplet states are present at the lowest energy, which justifies the presence of two different dynamics observed in the pump and probe experiments. Moreover, some mixing with a triplet state is found for example for the lowest singlet state. This shows that some small mixing of states with different multiplicity is present, and this agrees with the short decay time observed in the pump and probe experiments.

We have also calculated the triplet to triplet spectrum to account for the pump and probe experiments. Fc in the triplet state was fully optimized at ZORA, PBE level with small frozen core TZ2P basis set, and it was found to converge to a nearly C_{2v} geometry (see Figure 9). In the triplet state, the distance Fe-Cp increases to 1.80 Å. The Cp rings are tilted by 5° and exhibit a folding angle of 2.5°. In the singlet state, the H atoms are bent (1°) pointing toward iron, as already reported,[51] whereas in the triplet state, the H atoms are bent away from the metal (1−2°), except those bound to the out-of-Cp plane C atoms, which point toward iron (4°). The energy difference between S_0 and T_1 computed at ZORA, PBE TZ2P all electron level was found to be 1.63 eV (37.5 kcal mol^{-1}), a value in very good agreement with the experimental one.[6] We also calculated the triplet to triplet

TABLE 3: Excitation Energies Calculated for the PBE Optimized Geometry; Level of Theory: Spin Orbit ZORA, LB94 with TZ2P All Electron Basis Set[a]

exc state	energy		dominant states	band		exp
E_2''	2.82	singlet	$1E_2''(1)$ 0.98 (2.81 eV)	$7e_{5/2} \rightarrow 13e_{1/2}$	0.6266	2.81/2.70[a]
		triplet	$1E_2''(2)$ 0.02 (2.33 eV)	$8e_{3/2} \rightarrow 9e_{3/2}$	0.3713	
E_1''	2.91	singlet	$1E1''(1)$	$12e_{1/2} \rightarrow 9e_{3/2}$	0.4212	2.81/2.98[a]
				$12e_{1/2} \rightarrow 13e_{1/2}$	0.3587	
				$8e_{3/2} \rightarrow 13e_{1/2}$	0.1193	
				$7e_{5/2} \rightarrow 9e_{3/2}$	0.1001	
E_1''	3.44	singlet	$2E1''(1)$	$8e_{3/2} \rightarrow 13e_{1/2}$	0.4059	3.82/3.82[a]
				$7e_{5/2} \rightarrow 9e_{3/2}$	0.3691	
				$12e_{1/2} \rightarrow 9e_{3/2}$	0.1139	
				$12e_{1/2} \rightarrow 13e_{1/2}$	0.1053	
E_1'	2.31	triplet	$1E_2''(2)$ 0.50 (2.33 eV)	$7e_{5/2} \rightarrow 9e_{3/2}$	0.4998	2.34[a]
		triplet	$1E_2''(1)$ 0.50 (2.33 eV)	$7e_{3/2} \rightarrow 9e_{5/2}$	0.4998	
E_2'	2.36	triplet	$1E_2''(2)$ 0.50 (2.33 eV)	$8e_{3/2} \rightarrow 13e_{1/2}$	0.9978	2.34[a]
		triplet	$1E_2''(1)$ 0.50 (2.33 eV)	$11e_{1/2} \rightarrow 10e_{3/2}$	0.0004	

[a] From ref 8a. [a] All values are in eV.

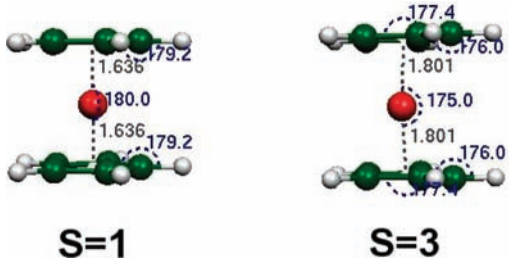

Figure 9. Geometry of ferrocene in singlet and triplet ground state. Level of theory: ZORA PBE TZ2P small core.

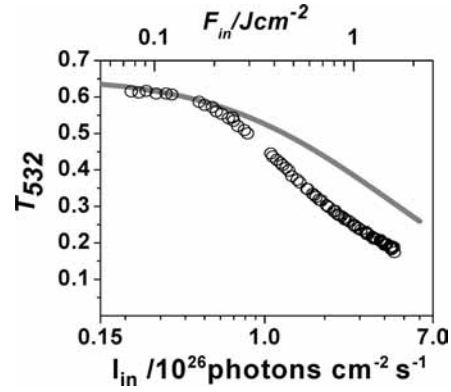

Figure 10. Nonlinear transmission vs incident fluence at 532 nm. Fitting (continuous line) of the experimental points (circles) has been generated with the model including one-photon excitation from ground singlet state and one-photon from the first excited triplet state.

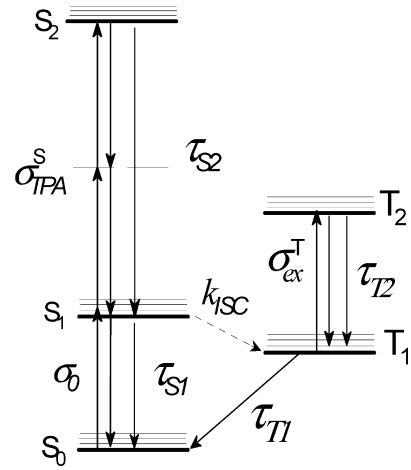

Figure 11. Model for the excited state dynamic of Fc with a two-photon absorption from the first excited singlet state.

spectrum and found that the first excited state is found at 4.9 eV (253 nm). This justifies the small differential optical density observed in the pump and probe spectrum with the presence of an increasing absorption at shorter wavelength than 500 nm and the absence of any peaks in the visible range (see Figure 5).

Therefore, calculations account for both the linear ground state optical spectrum and the pump and probe measurements in the nanosecond time regime.

From the transmission data reported in Figure 2, one finds that at low fluence (below 0.1 J cm^{-2}) Fc absorbs linearly. At higher fluences, one observes a decrease of transmission while pump and probe measurements show that a triplet to triplet absorption is present with an intersystem crossing quantum yield of 0.085. Without further data on the dynamic between the two lowest triplet states, we considered, with the aim of defining a model, that a triplet state is present with a lifetime of 90 ns, which is an average of the observed lifetimes of the two triplet states. The lifetime of the first excited singlet state of Fc was estimated from fluorescence lifetime measurement of the weak signal of Fc in methanol at 550 nm which was found to be 1.0 10^{-11} s.

Figure 10 shows the best fitting of the experimental nonlinear transmission data considering the one-photon absorption from the singlet ground state at 532 nm ($\sigma_0 = 2.2 \times 10^{-20}$ cm^2) and that of the triplet state at the same wavelength ($\sigma_T = 2.1\ 10^{-17}$ cm^{-2}).

The faster decrease of the transmission at high fluences with respect to the calculated one suggests that simultaneous absorption processes with more than one-photon should be present at this fluences. Models based on a sequential two-photon absorption from the ground state, which could be also important in an off-resonant situation,[56] cannot reproduce the observed nonlinear transmission. Therefore, we considered the occurrence of a two-photon absorption process starting either from an excited singlet or an excited triplet state. These types of multiphoton absorptions from excited states have been recently observed, using nanosecond pulses, in different molecular systems,[21,22] and derive from the large susceptibilities that excited states possess.

We found that the best model for fitting the experimental data is that described in Figure 11 where a simultaneous two-photon excitation from the first excited singlet state with absorption cross section σ^{S}_{TPA} is also considered.

For the model of Figure 11, the excited states population dynamic can be described with the following equations which can be numerically solved:[20]

$$\frac{dN_{S0}}{dt} = -\sigma_0 N_{S0} I_{in} + \sigma_0 N_{S1} I_{in} + \frac{N_{S1}}{\tau_{S1}} + \frac{N_{T1}}{\tau_{T1}} \quad (5a)$$

$$\frac{dN_{S1}}{dt} = \sigma_0 N_{S0} I_{in} - \sigma_0 N_{S1} I_{in} - \frac{N_{S1}}{\tau_{S1}} - k_{ISC} N_{S1} - \sigma^{S}_{TPA} N_{S1} I^2_{in} + \sigma^{S}_{TPA} N_{S2} I^2_{in} + \frac{N_{S2}}{\tau_{S2}} \quad (5b)$$

$$\frac{dN_{S2}}{dt} = -\sigma^{S}_{TPA} N_{S2} I^2_{in} + \sigma^{S}_{TPA} N_{S1} I^2_{in} - \frac{N_{S2}}{\tau_{S2}} \quad (5c)$$

$$\frac{dN_{T1}}{dt} = k_{ISC} N_{S1} - \sigma^{T}_{exc} N_{T1} I_{in} + \sigma^{T}_{exc} N_{T2} I_{in} - \frac{N_{T1}}{\tau_{T1}} + \frac{N_{T2}}{\tau_{T2}} \quad (5d)$$

$$\frac{dN_{T2}}{dt} = \sigma^{T}_{exc} N_{T1} I_{in} - \sigma^{T}_{exc} N_{T2} I_{in} - \frac{N_{T2}}{\tau_{T2}} \quad (5e)$$

In eqs 5a N_i are population densities, σ_i are absorption cross sections for one-photon (σ_0, σ^{T}_{exc}) and two-photon (σ^{S}_{TPA}) processes, k_{ISC} is the intersystem crossing rate constant, τ_i is the time constants for the relaxation processes, and I_{in} is the intensity of the input pulse in ph cm^{-2} s^{-1}. Considering a Gaussian temporal profile and top hat spatial profiles of the laser pulse, like the experimentally measured pulses used for the experiments, we calculated the nonlinear transmission using the population at different times obtained with the above equations and the photon propagation equation.[20] The fitting is reported in Figure 12 using the parameter values of Table 4. Fitting is shown using both the transmittance versus input intensities in a logarithmic scale and the output fluence versus input intensities in a linear scale. The first plot gives better evidence to the fitting in the low intensity region whereas the second one is to that in the high intensity region. One can see that the model calculation fits well both the low and the high intensity regions. The result shows that the two-photon absorption from excited singlet state is very important for the nonlinear absorption behavior of Fc.

One should observe the very high value of σ^{S}_{TPA} that is 4 to 5 order of magnitude larger than those usually found for two photon excitations from ground state. This result is characteristic of nonlinear processes from excited states which are very polarizable states.[57] One also observes the short lifetime of the first excited singlet state (10 ps) obtained by the fitting, which suggests further investigations in which rotational relaxation of this excited state is considered.

Conclusions

The linear and nonlinear absorption properties of Fc in toluene have been determined and analyzed. By using TD-DFT calculations, the linear optical properties of Fc have been revisited and accounted for. We found that Fc in toluene behaves as a reverse saturable absorber to nanosecond pulses at 532 nm. The excited triplet state of Fc has been observed and its physical properties determined with pump and probe experiments. Calculations also accounted for the observed spectrum of the excited triplet state of Fc. It has been found that fitting of nonlinear transmission could not be possible when only the dynamics of the triplet states is considered. We concluded that the model for the nonlinear absorption properties of Fc has to consider an additional two-photon absorption process from the first excited singlet state. Such absorption is characterized by having a large value of cross section (2.4 × 10^{-41} cm^4 s ph^{-1} mol^{-1}), typical of multiphoton absorption processes starting from excited states.

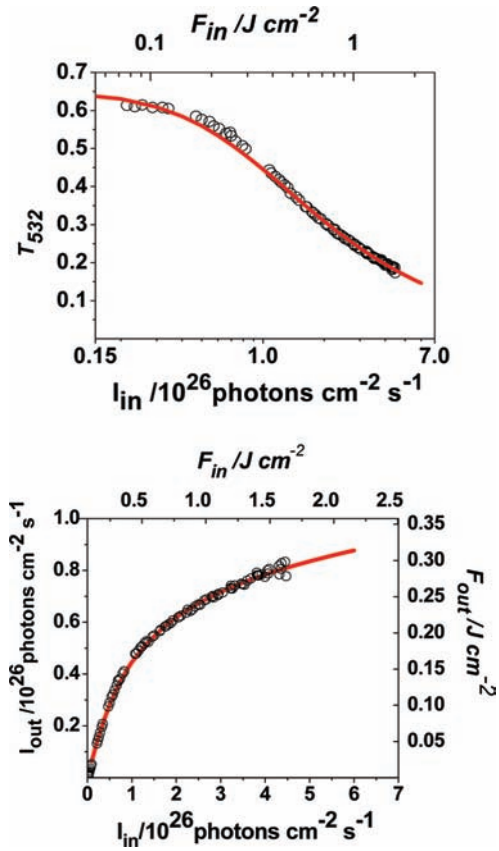

Figure 12. Plots of (upper) nonlinear transmission vs incident fluence (T_{532} vs F_{in}) and (lower) transmitted fluence (F_{out}) vs F_{in} for Fc in toluene at 532 nm. Fit (continuous line) of the experimental points (open circles) has been generated with the model of multiphoton absorption shown in Figure 11.

TABLE 4: Parameters Values for the Fitting of the Experimental Data in Figure 12

σ_0	2.2×10^{-20} cm^2	τ_{S1}	1.0×10^{-11}s
σ^{T}_{exc}	2.1×10^{-17} cm^2	τ_{S2}	9.1×10^{-13}s
σ^{S}_{TPA}	2.4×10^{-41} cm^4 s ph^{-1} mol^{-1}	τ_{T1}	9.0×10^{-8} s
k_{ISC}	8.5×10^{9} s^{-1}	τ_{T2}	1×10^{-12}s

Acknowledgment. Financial support by the University of Padova (PRAT n. CPDA063353) and the Ministry of University and Research (PRIN n. 2006034372) are acknowledged. We thank Francesco Enrichi for the fluorescence lifetime measurements, Gabriele Marcolongo and Simone Crivellaro for technical support.

References and Notes

(1) (a) Kealy, T. J.; Pauson, P. L. *Nature* **1951**, *168*, 1039. (b) Miller, S. A.; Tebboth, J. A.; Tremaine, J. F. *J. Chem. Soc.* 1952, *632*.

(2) (a) Wilkinson, G.; Rosenblum, M.; Whiting, M. C.; Woodward, R. B. *J. Am. Chem. Soc.* **1952**, *74*, 2125. (b) Eiland, P. F.; Pepinsky, R. *J. Am. Chem. Soc.* **1952**, *74*, 4971. (c) Dunitz, J. D.; Orgel, L. E. *Nature* **1953**, *177*, 121.

(3) Tarr, A. M.; Wiles, D. M. *Can. J. Chem.* **1968**, *46*, 2725.

(4) Bond, A. M.; Oldham, K. B.; Whiting, M. C.; Snook, G. A. *Anal. Chem.* **2000**, *72*, 3492.

(5) Astruc, D. In *Electron Transfer and Radical Processes in Transition-Metal Chemistry*; VCH: New York, 1995.

(6) (a) Fry, A. J.; Liu, R. S. H.; Hammond, G. S. *J. Am. Chem. Soc.* **1963**, *88*, 528. (b) Fry, A. J.; Liu, R. S. H.; Hammond, G. S. *J. Am. Chem. Soc.* **1966**, *88*, 4781. (c) Kikuchi, M.; Kikuchi, K.; Kokubun, H. *Bull. Chem. Soc. Jpn.* **1974**, *47*, 1331. (d) Farmilo, A.; Wilkinson, F. *Chem. Phys. Lett.* **1975**, *34*, 575. (e) Herkstroeter, W. G. *J. Am. Chem. Soc.* **1975**, *97*, 4161.

(7) (a) Xenogiannopolou, E.; Medved, M.; Iliopoulos, K.; Couris, S.; Papadopoulos, M. G.; Bonifazi, D.; Sooambar, C.; Mateo-Alonso, A.; Prato, M. *Chem. Phys. Chem.* **2007**, *8*, 1056. (b) Zheng, Q.; He, G. S.; Lu, C.; Prasad, P. N. *J. Mater. Chem.* **2005**, *15*, 3488. (c) Tsuboya, N.; Hamasaki, R.; Ito, M.; Mitsuishi, M.; Miyashita, T.; Yamamoto, Y. *J. Mater. Chem.* **2003**, *13*, 511. (d) Guldi, D. M.; Aminur Rahman, G. M.; Marczak, R.; Matsuo, Y.; Yamanaka, M.; Nakamura, E. *J. Am. Chem. Soc.* **2006**, *128*, 9420. (e) Gonzalez-Rodriguez, D.; Torres, T.; Olmstead, M. M.; Rivera, J.; Herranz, M. A.; Echegoyen, L.; Atienza-Castellanos, C.; Guldi, D. M. *J. Am. Chem. Soc.* **2006**, *128*, 10680. (f) Yang, F.; Xu, X. L.; Gong, Y. H.; Qiu, Z. R.; Sun, W. W.; Zhou, J. W.; Audebert, P.; Tang, J. *Tetrahedron* **2007**, *63*, 9188. (g) Li, J.; Song, Y.; Hou, H.; Tang, M.; Fan, Y.; Zhu, Y. *J. Organomet. Chem.* **2007**, *692*, 1584. (h) Misra, R.; Kumar, R.; Chandrashekar, T. K.; Suresh, C. H.; Nag, A.; Goswami, D. *J. Am. Chem. Soc.* **2006**, *128*, 16083. (i) Zhang, X. B.; Feng, J. K.; Ren, A. M.; Sun, C. C. *J. Phys. Chem. A* **2006**, *44*, 12222. (j) Alain, V.; Blanchard-Desce, M. C.; Chen, C. T.; Marder, S. R.; Fort, A.; Barzukas, M. *Synth. Met.* **1996**, *81*, 133. (k) Albota, M.; Belijonne, D.; Bredas, J. L.; Erlich, J. E.; Fu, J. Y.; Heikal, A. A.; Hess, S. E.; Kogej, T.; Levin, M. D.; Marder, S. R.; McCord-Maughon, D.; Perry, J. W.; Rockel, H.; Rumi, M.; Subramaniam, C.; Webb, W. W.; Wu, X. L.; Xu, C. *Science* **1998**, *281*, 1653. (l) Balavoine, G. G. A.; Daran, J. C.; Iftime, G.; Lacroix, P. G.; Manoury, E.; Delaire, J. A.; Maltey-Fanton, I.; Nakatani, K.; Di Bella, S. *Organometallics* **1999**, *18*, 21. (m) Hudson, R. D. A.; Asselberghs, I.; Clays, K.; Cuffe, L. P.; Gallagher, J. F.; Manning, A. R.; Persoons, A.; Wostyn, K. *J. Organomet. Chem.* **2001**, *435*, 637. (n) Zu, Y.; Wolf, M. O. *J. Am. Chem. Soc.* **2000**, *122*, 10121. (o) Guldi, D. M.; Maggini, M.; Scorrano, G.; Prato, M. *J. Am. Chem. Soc.* **1997**, *119*, 974. (p) Kubo, M.; Mori, Y.; Otani, M.; Murakami, M.; Ishibashi, Y.; Yasuda, M.; Hosomizu, K.; Miyasaka, H.; Imahori, H.; Nakashima, S. *J.Phys.Chem. A* **2007**, *111*, 5136.

(8) (a) Sohn, Y. S.; Hendrickson, D. N.; Gray, H. B. *J. Am. Chem. Soc.* **1971**, *93*, 3603. (b) Gordon, K. R.; Warren, K. D. *Inorg. Chem.* **1978**, *17*, 987.

(9) Jaworska-Augustyniak, A.; Karolczak, J.; Maciejewski, A.; Wojtczak, J. *Chem. Phys. Lett.* **1987**, *137*, 134.

(10) Görner, H.; D. Sculte-Frohlinde, D. *J. Photochem.* **1981**, *16*, 169.

(11) Maciejewski, A.; Jaworska-Augustyniak, A.; Szeluga, Z.; Wojtczak, J.; Karolczak, J. *Chem. Phys. Lett.* **1988**, *153*, 227.

(12) Scott, D. R.; Becker, R. S. *J. Chem. Phys.* **1961**, *35*, 516.

(13) Smith, J. J.; Meyer, B. *J. Chem. Phys.* **1968**, *48*, 5436.

(14) Müller-Goldegg, A.; Voigtländer, J. *Z. Naturforsch. A* **1968**, *23*, 1236.

(15) Schandry, R.; Voigtländer, J. *Z. Naturforsch. A* **1971**, *26*, 1772.

(16) (a) Whitall, I. R.; McDonagh, A. M.; Humphrey, M. G. *Adv. Organomet. Chem.* **1998**, *42*, 291. (b) Verbiest, T.; Houbrechts, S.; Kauranen, M.; Clays, K.; Persoons, A. *J. Mater. Chem.* **1997**, *7*, 2175.

(17) (a) Araki, Y.; Yasumura, Y.; Ito, O. *J. Phys. Chem. B* **2005**, *109*, 9843. (b) Figueira-Duarte, T. M.; Rio, Y.; Listorti, A.; Delavaux-Nicot, B.; Holler, M.; Marchioni, F.; Ceroni, P.; Armaroli, N.; Nierengarten, J. *New J. Chem.* **2008**, *32*, 54.

(18) Bensasson, R.; Goldschmidt, C. R.; Land, E. J.; Truscott, T. G. *Photochem. Photobiol.* **1978**, *28*, 277.

(19) Casida, M. E.; Jamorski, C.; Casida, K. C.; Salahub, D. R. *J. Chem. Phys.* **1998**, *108*, 4439.

(20) Ehlert, J.; Stiel, H.; Teuchner, K. *Comput. Phys. Commun.* **2000**, *124*, 330.

(21) Dini, D.; Calvete, M. J. F.; Hanack, M.; Amendola, V.; Meneghetti, M. *J. Am. Chem. Soc.* **2008**, *130*, 12290.

(22) (a) Schiccheri, N.; Meneghetti, M. *J. Phys. Chem. A* **2005**, *109*, 4643. (b) Villano, M.; V. Amendola, V.; Sandonà, G.; Donzello, M. P.; Ercolani, C.; Meneghetti, M. *J. Phys. Chem. B* **2006**, *110*, 24354.

(23) Baerends, E. J.; Autschbach, J.; Bérces, A.; Berger, J. A.; Bickelhaupt, F. M. Bo, C.; de Boeij, P. L.; Boerrigter, P. M.; Cavallo, L.; Chong, D. P.; Deng, L.; Dickson, R. M.; Ellis, D. E.; van Faassen, M.; Fan, L.; Fischer, T. H.; Fonseca Guerra, C.; Van Gisbergen, S. J. A.; Groeneveld, J. A.; Gritsenko, O. V.; Grüning, M.; Harris, F. E.; Van den Hoek, P.; Jacob, C. R.; Jacobsen, H.; Jensen, L.; Kadantsev, E. S.; Van Kessel, G.; Klooster, R.; Kootstra, F.; Van Lenthe, E.; McCormack, D.A. Michalak, A.; Neugebauer, J.; Nicu, V. P.; Osinga, V. P.; Patchkovskii, S.; Philipsen, P. H. T.; Post, D.; Pye, C. C.; Ravenek, W.; Romaniello, P.; Ros, P.; Schipper, P. R. T.; Schreckenbach, G.; Snijders, J. G.; Solà, M.; Swart, M.; Swerhone, D.; Te Velde G.; Vernooijs, P.; Versluis, L.; Visscher, L.; Visser, O.; Wang, F.; Wesolowski, T. A.; Van Wezenbeek, E. M.; Wiesenekker, G.; Wolff, S. K.; Woo, T. K.; Yakovlev, A. L.; Ziegler, T. *ADF 2007. 01*; SCM: Amsterdam, 2007.

(24) Van Lenthe, E.; Baerends, E. J. *J. Comput. Chem.* **2003**, *24*, 1142.

(25) Te Velde, G.; Bickelhaupt, F. M.; Baerends, E. J.; Fonseca Guerra, C.; van Gisbergen, S. J. A.; Snijders, J. G.; Ziegler, T. *J. Comput. Chem.* **2001**, *21*, 931.

(26) Van Lenthe, E.; Baerends, E. J.; Snijders, J. G. *J. Chem. Phys.* **1993**, *99*, 4597.

(27) Vosko, S. H.; Wilk, L.; Nusair, M. *Can. J. Phys.* **1980**, *58*, 1200.

(28) Becke, A. D. *Phys. Rev. A* **1988**, *38*, 3098.

(29) Lee, C.; Yang, W.; Parr, R. G. *Phys. Rev. B* **1988**, *37*, 785.

(30) Perdew, J. P.; Burke, K.; Ernzerhof, M. *Phys. Rev. Lett.* **1996**, *77*, 3865.

(31) Swart, M.; Ehlers, A. W.; Lammertsma, K. *Mol. Phys.* **2004**, *102*, 2467.

(32) Handy, N. C.; Cohen, A. *J. Mol. Phys.* **2001**, *99*, 403.

(33) Wang, F.; Ziegler, T.; Van Lenthe, E.; Van Gisbergen, S.; Baerends, E. J. *J. Chem. Phys.* **2005**, *122*, 204103.

(34) Van Leeuwen, R.; Baerends, E. *J. Phys. Rev. A* **1994**, *49*, 2421.

(35) (a) Blau, W.; Byrne, H.; Dennis, W. M.; Kelly, J. M. *Opt. Commun.* **1985**, *56*, 25. (b) Harter, D. J.; Shand, M. L.; Band, Y. B. *J. Appl. Phys.* **1984**, *56*, 865. (c) Giuliano, C. R.; Hess, L. D. *IEEE J. Quantum Electr.* **1967**, *QE-3*, 358.

(36) (a) Dini, D.; Barthel, M.; Schneider, T.; Ottmar, M.; Verma, S.; Hanack, M. *Solid State Ionics* **2003**, *165*, 289. (b) Dini, D.; Vagin, S.; Hanack, M.; Amendola, V.; Meneghetti, M. *Chem. Commun.* **2005**, 3796. (c) Dini, D.; Calvete, M. J. F.; Hanack, M.; Chen, W.; Ji, W. *ARKIVOC* **2006**, *3*, 77. (d) Zhang, Q. F.; Yu, Z.; Ding, J.; Song, Y.; Rothenberger, A.; Fenske, D.; Leung, W. H. *Inorg. Chem.* **2006**, *45*, 5187. (e) Ji, W.; Xie, W.; Tang, S. H.; Shi, S. *Mater. Chem. Phys.* **1996**, *43*, 45. (f) Francois, L.; Mostafavi, M.; Belloni, J.; Delouis, J. F.; Delaire, J.; Feneyrou, P. *J. Phys. Chem. B* **2000**, *104*, 6133. (g) Li, H. H.; Chen, Z. R.; Li, J. Q.; Huang, C. C.; Hu, X. L.; Zhao, B.; Ni, Z. X. *J. Cluster Sci.* **2005**, *16*, 537. (h) Li, H. H.; Chen, Z. R.; Li, J. Q.; Huang, C. C.; Zhang, Y. F.; Jia, G. X. *Eur. J. Inorg. Chem.* **2006**, 2447. (i) Kiran, P. P.; Bhakta, B. N. S.; Rao, D. N.; De, G. *J. Appl. Phys.* **2004**, *96*, 6717. (j) Dini, D.; Calvete, M. J. F.; Hanack, M.; Pong, R. G. S.; Flom, S. R.; Shirk, J. S. *J. Phys. Chem. B* **2006**, *110*, 12230.

(37) (a) Dini, D.; Hanack, M.; Meneghetti, M. *J. Phys. Chem. B* **2005**, *109*, 12691. (b) Donzello, M. P.; Ou, Z.; Dini, D.; Meneghetti, M.; Ercolani, C.; Kadish, K. M. *Inorg. Chem.* **2004**, *43*, 8637.

(38) (a) Pan, H.; Chen, W.; Feng, Y. P.; Ji, W.; Lin, J. *Appl. Phys. Lett.* **2006**, *88*, 223106. (b) Fu, S.; Zhu, X.; Wong, W. Y.; Ye, C.; Wong, W. K.; Li, Z. *Eur. J. Inorg. Chem.* **2007**, 2004. (c) Vincent, D. *Appl. Opt.* **2001**, *40*, 6646.

(39) Tutt, L. W.; Kost, A. *Nature* **1992**, *356*, 225.

(40) Bensasson, R.; Land, E. J. *Trans. Faraday Soc.* **1971**, *67*, 1904.

(41) Rhys Williams, A. T.; Winfield, S. A.; Miller, J. N. *Analyst* **1983**, *108*, 1067.

(42) Fleming, G. R.; Knight, A. W. E.; Morris, J. M.; Morrison, R. J. S.; Robinson, G. W. *J. Am. Chem. Soc.* **1976**, *99*, 4306.

(43) Mittal, J. P. *Pure Appl. Chem.* **1995**, *67*, 103.

(44) (a) Stephenson, P. B. *J. Chem. Phys.* **1971**, *55*, 473. (b) Armstrong, A. T.; Smith, F.; Elder, E.; McGlynn, S. P. *J. Chem. Phys.* **1967**, *46*, 4321. (c) Stephenson, P. B.; Winterrowd, W. E. *J. Chem. Phys.* **1970**, *52*, 3308. (d) Sohn, Y. S.; Hendrickson, D. N.; Smith, J. H.; Gray, H. B. *Chem. Phys. Lett.* **1970**, *6*, 499. (e) Rohmer, M. M.; Veillard, A.; Wood, M. H. *Chem. Phys. Lett.* **1974**, *29*, 466. (f) Armstrong, D. R.; Fortune, R.; Perkins, P. G. *J. Organomet. Chem.* **1976**, *111*, 197. (g) Kaplan, L.; Kester, W. L.; Katz, J. J. *J. Am. Chem. Soc.* **1952**, *74*, 5531. (h) Brand, J. C. D.; Snedden, W. *Trans. Faraday Soc.* **1957**, *53*, 894.

(45) (a) Moffitt, W. E. *J. Am. Chem. Soc.* **1954**, *76*, 3386. (b) Dunitz, J. D.; Orgel, L. E. *J. Chem. Phys.* **1955**, *23*, 954. (c) Yamazaki, M. *J. Chem. Phys.* **1956**, *24*, 1260.

(46) (a) Luthi, H. P.; Ammeter, J. H.; Almlof, J.; Faegri, K., Jr. *J. Chem. Phys.* **1982**, *77*, 2002. (b) Rösch, N.; Jörg, H. *J. Chem. Phys.* **1986**, *84*, 5967. (c) Park, C.; Almlof, J. *J. Chem. Phys.* **1991**, *95*, 1829.

(47) (a) Bohn, R. K.; Haaland, A. *J. Organomet. Chem.* **1966**, *5*, 470. (b) Haaland, A.; Nilsson, J. E. *Acta Chem. Scand.* **1968**, *22*, 2653. (c) Haaland, A.; Lusztyk, J.; Novak, D. P.; Brunvoll, J.; Starowieyski, K. B. *J. Chem. Soc., Chem. Commun.* 1974, *54*. (d) Dunitz, J. D.; Orgel, L. E.; Rich, A. *Acta Crystallogr., Sect. B* **1956**, *9*, 373. (e) Seiler, P.; Dunitz,

J. D. *Acta Crystallogr., Sect. B* **1979**, *35*, 2020. (f) Takusagawa, F.; Koetzle, T. F. *Acta Crystallogr., Sect. B* **1979**, *35*, 1074.

(48) Rosa, A.; Ricciardi, G.; Gritsenko, O.; Baerends, E. J. *Struct. Bonding (Berlin)* **2004**, *112*, 49.

(49) Coriani, S.; Haaland, A.; Helgaker, T.; Jorgensen, P. *Chem. Phys. Chem.* **2006**, *7*, 245.

(50) Elschenbroich, C.; Salzer, A. In *Organometallics: A Concise Introduction, 2nd Ed.;* VCH: Germany, 1992.

(51) Swart, M. *Inorg. Chim. Acta* **2007**, *360*, 179.

(52) Armstrong, A. T.; Carroll, D. G.; McGlynn, S. P. *J. Chem. Phys.* **1967**, *47*, 1104.

(53) Rohmer, M. M.; Veillard, A.; Wood, M. H. *Chem. Phys. Lett.* **1974**, *29*, 466.

(54) Boulet, P.; Chermette, H.; Daul, C.; Gilardoni, F.; Rogemond, F.; Weber, J.; Zuber, G. *J. Phys. Chem. A* **2001**, *105*, 885.

(55) Rudberg, E.; Salek, P.; Helgaker, T.; Agren, H. *J. Chem. Phys.* **2005**, *123*, 184108.

(56) Baev, A.; Salek, P.; Gel'mukhanov, F.; Agren, H. *J. Phys. Chem. B* **2006**, *110*, 5379.

(57) Lower, S. K.; El-Sayed, M. A. *Chem. Rev.* **1966**, *66*, 199.

JP9047192